CARBONATE NMR PERMEABILITY ESTIMATES BASED ON THE WINLAND-PITTMAN MICP APPROACH

Edmilson Helton Rios, National Observatory; Adam Keith Moss, Timothy Neil Pritchard, Ana Beatriz Guedes Domingues, BG Group plc.; Rodrigo Bagueira de Vasconcellos Azeredo, Fluminense Federal University

ABSTRACT

Nuclear magnetic resonance (NMR) logging is widely used for continuous downhole permeability estimates. But long before NMR, laboratory measurements of capillary pressure curves were used for the same purpose. Remarkably, the mercury injection capillary pressure (MICP) technique was developed for predicting the permeability of small and irregular-shaped samples, such as drilling cuts. In the Winland-Pittman MICP approach, pore-throat radii corresponding to different Hg saturations were individually correlated with porosity and permeability. The saturation where the best correlation is found defines the critical aperture. By adapting this methodology for NMR context, this work introduces a novel concept of cumulative saturation cutoff applied on the transverse relaxation time (T_2) distributions. The performance and the fitting coefficient as a function of saturation cutoff were graphically analyzed for a group of North Sea and Middle East Carbonate core plugs. Critical saturation cutoffs for both pure and size-scaled NMR distributions delivered better permeability estimates when compared with the standard logarithmic mean estimator.

INTRODUCTION

Kozeny developed a theory, later improved by Carman, in which porous rocks are regarded as bundles of capillary tubes [1]. The so-called Kozeny-Carman equation takes many forms, including the following:

$$k_{kc} = a' \phi_b \left(\frac{V}{S}\right)^c,$$ (1)

where a', b and c are general coefficients for adjustment, ϕ is porosity, V/S is volume-to-surface-area ratio, also known as the hydraulic radius. For simple pore geometries, V/S can be written as R_p/γ, where R_p is the pore radius and γ is a pore shape factor (e.g. 1 represents flat or flake-like pores, 2 represents open-ended cylindrical pores and 3 represents spherical pores). From Equation 1, Winland [2] and then Pittman [3] related MICP-derived pore-throat radius R_t with permeability and porosity, as following:

$$logR_t = a_1 logk + a_2 log\phi + a_3,$$ (2)

where $a_1 = 1/c$, $a_2 = -b/c$ and $a_3 = (\log a')/c + log(\delta/\gamma)$, with δ being the

pore body-to-throat ratio (R_p/R_t). $R_t = -2\sigma cos\theta/P_c$, with σ and θ being the air-mercury interfacial tension and the surface contact angle, respectively, and P_c is the capillary pressure, selected for a specific saturation of the MICP curve $S(P_c)$. The best-performing correlation defines the aperture that best describes permeability.

Seevers [4] and then Kenyon [5] showed that nuclear magnetic resonance (NMR) porosity and an average of the longitudinal T_1 or transverse T_2 NMR relaxation times could be indirectly used as the independent variables of Equation 1 if considered the fast diffusion regime and assuming no diffusional relaxation effects due to magnetic field gradients nor diffusion pore coupling [6]. The Seevers-Kenyon NMR estimator can be written for T_2 (the widely used in modern NMR logging) as follows:

$$k_{SK} = a\phi_{NMR}^b(T_{2lm})^c, \tag{3}$$

where $a = a'\rho_2^c$ is a pre-multiplier factor that includes the T_2 surface relaxivity (ρ_2), $\phi_{NMR} = \sum \phi(T_2)$ is the NMR-derived total porosity and $T_{2lm} \approx (1/\rho_2)(V/S)$ is the logarithmic mean of the $\phi(T_2)$ distribution such that $T_{2lm}^{\phi_{NMR}} = \prod T_2^{\phi(T_2)}$. Literature coefficients are commonly used in the logging suites under an estimator usually called as Schlumberger-Doll-Research model, $k_{SDR} = a\phi_{NMR}^4 T_{2lm}^2$. In this work, the Winland-Pittman approach was adapted for the NMR context as follows:

$$k_{sat} = a\phi_{NMR}^b(T_{2sat})^c, \tag{4}$$

where $a = a'\rho_2^c = (10^{a_3}\rho_2 \gamma/\delta)^c$, $b = -a_2 c$ and $c = 1/a_1$ are fitting coefficients, the T_{2sat} is a relaxation time selected for a fixed point in the cumulative saturation curve. The saturation cutoff is applied to the cumulative curves computed from the normalized (or saturation-based) NMR distributions $S(T_2)$, such that $\sum S(T_2) = 1$. Several cutoffs are tested using Equation 6 and the sat-based estimates are compared to the standard k_{SK} estimator.

NMR carbonates are generally less sensitive to variations in pore body size, thus T_2 distributions were size-scaled based on a NMR-MICP data integration. Because true surface relaxivity is very complex to be determined and depends on the method used, a simple scaling factor defined as the ratio of the logarithmic means between MICP and NMR distributions were employed. This size-scaling factor encompasses both the surface relaxivity and the geometry of the pore system (both assumed to be constant within all pore-size families) as follows:

$$S_{MICP} \equiv \frac{R_{tlm}}{T_{2lm}} \approx \frac{R_{plm}/\delta}{R_{plm}/\gamma\rho_2} = \frac{\gamma}{\delta}\rho_2, \tag{5}$$

where R_{plm} is the logarithmic mean of the pore radius distribution, γ is a pore shape factor for simple geometries and δ is the pore body-to-throat ratio. By solving for ρ_2 in Equation 5 and inserting it into Equations 3 and 4, size-scaled NMR permeability estimators can be obtained where the pre-multiplier a incorporates the geometry of the pore system such that $a = a'(\delta/\gamma)^c$.

EXPERIMENTAL

Carbonates rocks from Cretaceous chalk fields were studied: 14 from Norwegian reservoirs in North Sea (the Valhall, Hod and Tommeliten fields) and 15 diagenetic chalks from Middle East (the Thamama C Formation, Bu Hasa Field, Abu Dhabi). Core plugs (1.5' x 1.8') and small core-end trims (visually representative of the plugs) were cleaned of native fluids via Soxhlet extraction and then dried in an oven [7]. The MICP measurements were performed in an AutoPore II 9220, with a "filling pressure" of 0.1 bar followed by one hundred pressure steps with maximum pressure of 4,130 bar. Plugs were routine core analysed (RCAL) using helium gas at an overburden pressure of 20 bars and then they were fully saturated with a 50,000 ppm brine solution for NMR measurements. The ^{1}H NMR T_2 measurements of core samples were performed on a bench-top NMR analyzer at 2 MHz and 30°C using the Carr–Purcell–Meiboom–Gill (CPMG) technique [8], with 4,050 spin echoes spaced by 700 µs (Te). Under sufficient time for fully spin polarization 10s (Tw), signal averages were performed until a minimal signal-to-noise ratio (SNR) of 100. A distribution window with one hundred relaxation-time bins logarithmically spaced from 0.1 to 10,000 ms was set for T_2.

RESULTS

The normalized MICP, NMR, and size-scaled NMR distributions are shown on Figure 1a, b and c, respectively. Left side is the incremental curves and right side is the cumulative curves (two saturation cutoffs are showed as examples), respectively. For MICP and size-scaled NMR, micro-, meso- and macro-porosity ranges are outlined with the 0.3 and 3 µm threshold, in accordance with [9]. All the curves are labelled based on the increasing k_{RCAL} values of the plugs. Small apertures and pores corresponds to plugs with low k_{RCAL} (predominantly North Sea Chalks), whereas large apertures and pores corresponds to plugs with high k_{RCAL} (predominantly Middle East Chalks). The similarity between routine and special core analysed porosity in Figure 2a, indicates that gas, Hg and brine probed representative pore spaces and that isolated fluid-filled pores may not have been present. Figure 2b well illustrate that a simple power regression cannot simultaneously handle the different pore-perm trends exhibited by the chalk groups. Additional information such as apertures and pore sizes may help in obtaining a global permeability estimator.

The r-squared and the fitting coefficients for the estimators k_{SK} and k_{sat} (with 50 and 85%) are presented in Table 1 for pure and size-scaled T_2. Figure 3 plots the R-square and multiple linear regression coefficients obtained with saturation cutoffs from 5 to 85% under increments of 5%. The y-axis lower limit (0.37) corresponds to the particular case where coefficient c is null (Figure 2b). The performance of k_{SK} for each case is also indicated in the plot. Size scaling improved permeability estimation considerably for all case, producing lower b (for porosity) and higher c (for

$S_{MICP}T_2$) coefficients values. It indicates that the size-scaled T_2 distributions are more effective to explain permeability and maybe can mitigate some of the difficulties encountered in carbonate NMR, such as variations in surface relaxivity and diffusive pore coupling. Figure 5 shows the response curves for the k_{sk} and $k_{85\%}$ before and after size scaling. In their original works with sandstones, Winland and Pittman described an equivalent cumulative saturation (from micro to macro) of 65% and 75%, respectively.

CONCLUSION
Inspired by the work of Winland and Pittman on MICP data, a novel NMR permeability estimator was introduced based on new concept of cumulative saturation cutoffs. T_2 associated with macroporosity reveal much better results than the standard T_2 logarithmic mean estimator. To overcome the lower sensitivity of carbonate NMR to pore and throat variation, this new approach was also evaluated after T_2 distribution size scaling. The results exceeded the performance compared to the estimators with pure T_2. The study confirms the potentiality of saturation-based NMR permeability estimator and further evaluation is in course for logging application.

ACKNOWLEDGEMENTS

REFERENCES
1. Carman, P.C., 1956. Flow of gases through porous media, Butterworths Scientific Publications, London.
2. Kolodzie Jr., S., 1980, Analysis of pore throat size and use of the Waxman–Smits equation to determine OOIP in spindle field, Colorado, SPE 55th Annual Fall Technical Conference.
3. Pittman, E.D., 1992. Relationship of porosity and permeability to various parameters derived from mercury injection-capillary pressure curves for sandstone, American Association of Petroleum Geologists, 76 (2), 191–198.
4. Seevers, D.O., 1966. A nuclear magnetic method for determining the permeability of sandstones, Trans. 7th Ann. SPWLA Logging Symp.,Tulsa.
5. Kenyon, W.E., 1992. Nuclear magnetic resonance as a petrophysical measurement, Nucl. Geophys., 6(2), 153-171.
6. Dunn, K.J., Bergman, D.J. & Latorraca, G.A., 2002. Nuclear Magnetic Resonance—Petrophysical and Logging Applications, Pergamon Press, Oxford.
7. American Petroleum Institute, 1998. Recommended Practice for Core Analysis Procedure, 2nd edn, API RP 40, (Washington, DC:API)

8. Meiboom, S. & Gill D., 1958. Modified spin-echo method for measuring nuclear relaxation times, Rev. Scien. Inst., 29, 688-691, doi:10.1063/1.1716296.
9. Marzouk, I., Takezaki, H., & Suzuki, M., 1998. New classification of carbonate rocks for reservoir characterization, 8th SPE Inter. Petrol. Exhib. Confer.,10p

Table 1: Performance and regression coefficients for pure and size-scaled NMR permeability estimators.

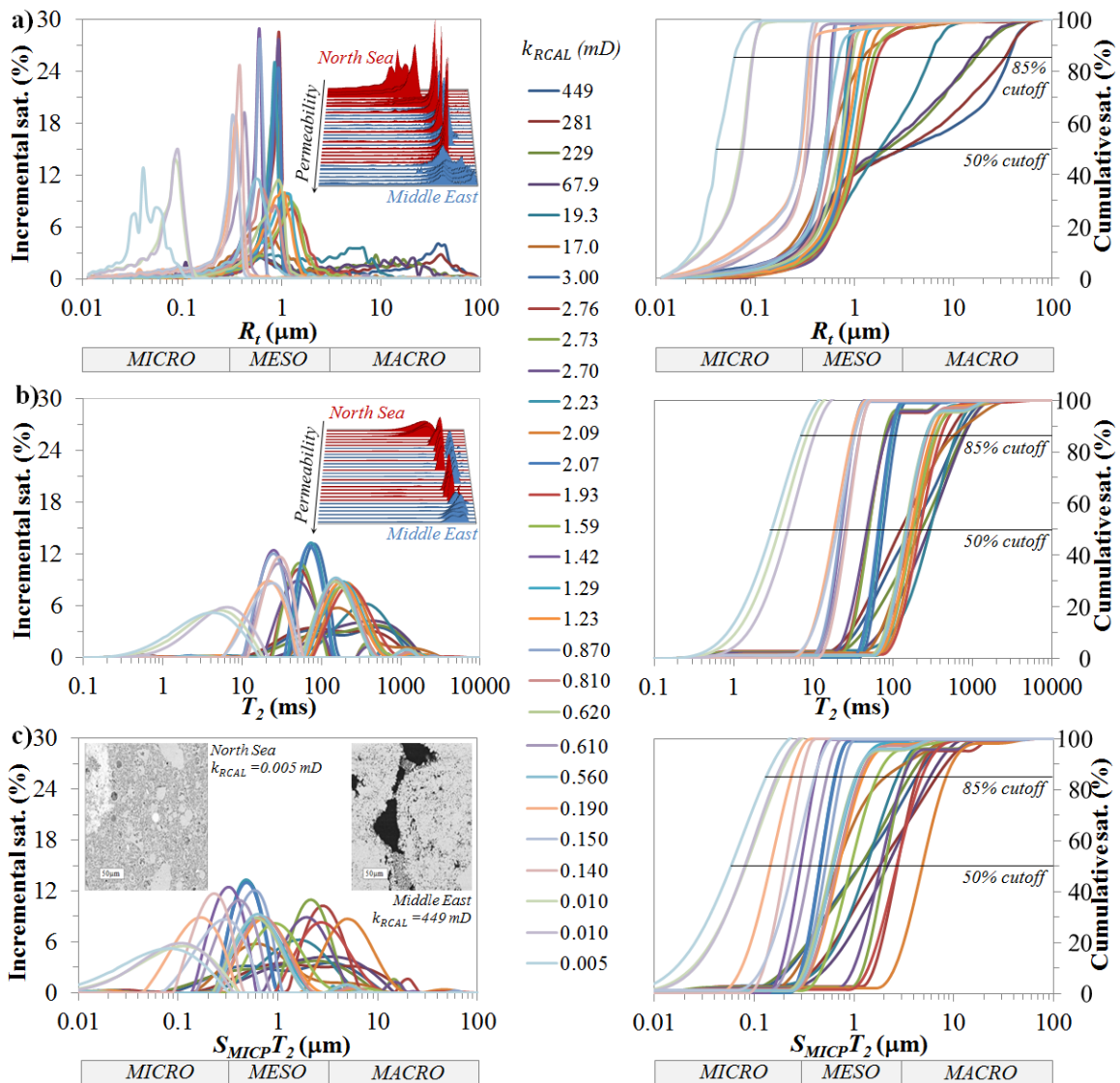| k_{NMR}	Pure T_2				Size-scaled T_2			
	R^2	a	b	c	R^2	a	b	c
k_{SK}	0.70	4E-05	2.82	1.33	0.89	7.65	0.01	2.54
$k_{50\%}$	0.71	3E-05	2.76	1.35	0.88	7.65	-0.04	2.53
$k_{85\%}$	0.81	1E-05	2.87	1.37	0.95	7.14	1.01	2.10

Figure 1: a) $S(R_t)$ and b) $S(T_2)$ with 3D plots showing each chalk group as inserts. c) Size-scaled NMR distribution $S(S_{MICP}T_2)$ with the thin section of the lower and higher permeability chalks as inserts.
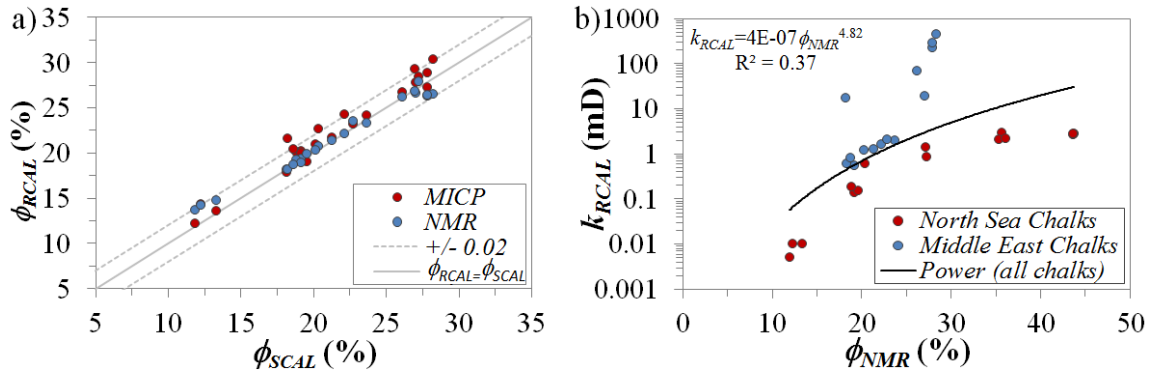
Figure 2: a) Routine core analysed porosity (standard reference) versus special core analysed porosities (MICP & NMR). b) RCAL permeability (standard reference) versus NMR porosity.
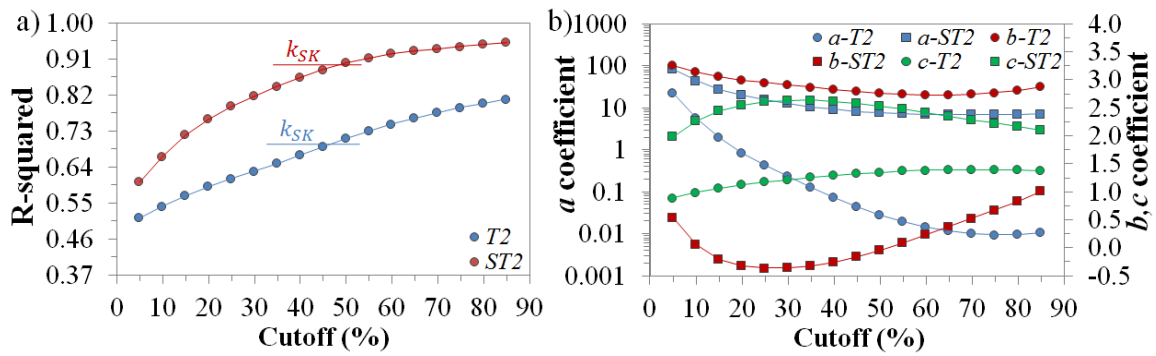

Figure 3: a) Performance and b) regression coefficients of the saturation-based estimator for both pure and size-scaled T_2 distribution.
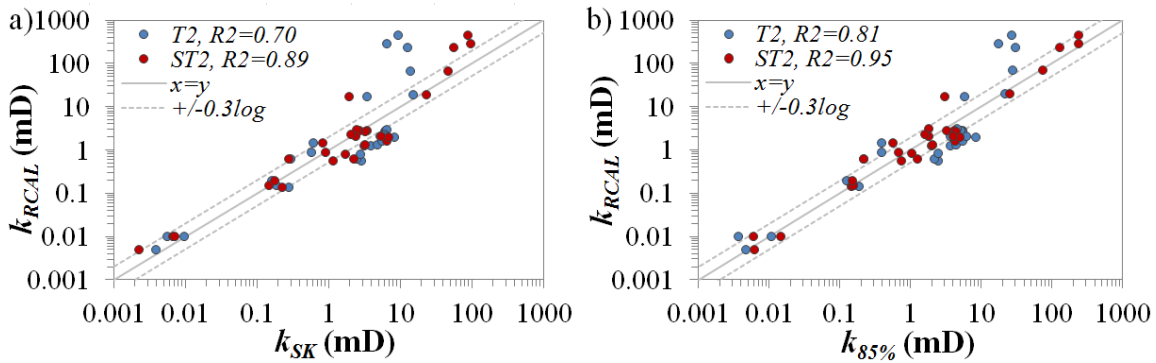

Figure 4: a) Standard log mean estimator and b) the best saturation−based estimator response curves.